Testing of Josephson array antennas and trim currents tuning[*]

A.A. Abdumalikov, P. Caputo[†] and A. V. Ustinov

Physikalisches Institut III, Universität Erlangen-Nürnberg
D-91054 Erlangen, Germany

[†] Current address: Universita' degli Studi di Salerno Dipartimento di Fisica Via. S. Allende,
I-84081 Baronissi (Salerno) Italy

September 2000

REPORT DOCUMENTATION PAGE

Form Approved OMB No. 0704-0188

1. REPORT DATE (DD-MM-YYYY) 20-11-2002	2. REPORT TYPE Final Report	3. DATES COVERED (From – To) 29 August 2000 - 29-Aug-01

4. TITLE AND SUBTITLE

Testing of Josephson Array Antennas and Trim Current Tuning

5a. CONTRACT NUMBER
F61775-00-C0004

5b. GRANT NUMBER

5c. PROGRAM ELEMENT NUMBER

6. AUTHOR(S)

A.A. Abdumalikov and A. V. Ustinov

5d. PROJECT NUMBER

5d. TASK NUMBER

5e. WORK UNIT NUMBER

7. PERFORMING ORGANIZATION NAME(S) AND ADDRESS(ES)
University of Erlangen-Nuremberg
Erwin-Rommel-Str. 1
Erlangen 91058
Germany

8. PERFORMING ORGANIZATION REPORT NUMBER

N/A

9. SPONSORING/MONITORING AGENCY NAME(S) AND ADDRESS(ES)

EOARD
PSC 802 BOX 14
FPO 09499-0014

10. SPONSOR/MONITOR'S ACRONYM(S)

11. SPONSOR/MONITOR'S REPORT NUMBER(S)
SPC 00-4046

12. DISTRIBUTION/AVAILABILITY STATEMENT

Approved for public release; distribution is unlimited.

13. SUPPLEMENTARY NOTES

14. ABSTRACT

This report results from a contract tasking University of Erlangen-Nuremberg as follows: contractor will investigate novel designs of triangular Josephson Junction arrays attempting to improve the high-frequency performance of the arrays in two ways; first, increase the operation frequencies and second, increase the output power of the millimeter-band radiation to level enabling practical application of the arrays. Three approaches will be investigated. First, trimming of currents at the array edges is expected to stabilize coherent oscillations and increase the operation margins (output power). Second, it appears promising to set up a traveling wave in a transmission line that contains an array comparable with the wavelength. Third, testing dipole-like active antennas to couple radiation out from arrays is a high priority task for emission in free space at high frequencies.

The contractor will experimentally verify the above concepts by designing new circuits and performing experiments with Nb/AOx/Nb Josephson Junction arrays. For these experiments, the contractor will use a millimeter-wave band receiver as well an on-chip detection circuits up to 300 GHz. Spatially-resolved measurements using low temperature scanning laser microscopy will be performed in order to monitor array dynamics at the junction level. Furthermore, the contractor intends to design a dipole antenna and test it with an integrated receiver in 400-500 GHz frequency range. For this purpose, improvements for a flux-flow oscillator as a local oscillator may be needed. Finally, the contractor will perform experiments with shunted junction arrays in order to simulate intrinsically overdamped high-Tc junctions and explore a possibility of using high Tc layered junctions for oscillator application

15. SUBJECT TERMS
EOARD, Josephson junctions, Millimeterwave technology, Microwave source

16. SECURITY CLASSIFICATION OF:			17. LIMITATION OF ABSTRACT	18, NUMBER OF PAGES	19a. NAME OF RESPONSIBLE PERSON Christopher Reuter, Ph. D.
a. REPORT UNCLAS	b. ABSTRACT UNCLAS	c. THIS PAGE UNCLAS	UL	30	19b. TELEPHONE NUMBER (Include area code) +44 +44 207 514 4474

Standard Form 298 (Rev. 8/98)
Prescribed by ANSI Std. Z39-18

Contents

Abstract

We have experimentally investigated the dynamics of triangular arrays of shunted Josephson junctions in a perpendicular magnetic field. By breaking symmetry of the array from cell to cell it is possible to increase flatness of the phases profile. Yukon and Lin proposed to do that by superimposing additional currents at the edges of the array. The currents trimming is expected to stabilize coherent oscillations at the same phase and increase the operation margins and emitting radiation power. These statements are true if the polarities of the bias and trim currents are opposite. Otherwise the operation margins and emitting radiation power will be decreased. Within current project we have designed a new circuitry to verify above statements. We have measured the dc-characteristics of the square cell triangular arrays. First measurements of these circuits are presented in this report.

Chapter 1

Introduction

While Josephson junctions provide compact tunable source of radiation in mm and sub-mm frequency range, their main drawback has been low rf power output per junction. In order to use this power in practical applications one should collect coherent radiation from many junctions coupled in arrays [1]. Triangular arrays of Josephson junctions operating in an applied magnetic field have been proposed for obtaining useful radiation power in mm and sub-mm ranges [2, 3, 4]. At the applied field corresponding to half a flux quantum in every cell ($f = 0.5$), the junctions transverse to the forcing current oscillate about their equilibrium state rather than rotating over 2π, yielding an rf power with very small content of higher harmonics. Numerical simulations have shown that the entire array operating near the resonant frequency $\omega_{LC/3}$ can be phase locked, allowing maximum rf power to be generated. Previous experiments with triangular rows [5, 6, 7] have already demonstrated radiation from the *horizontal* junctions, although they are not subjected to the driving force from the external bias current. The radiation frequency is equal to the Josephson frequency of the *vertical* junctions.

In the symmetrically-biased systems the phase profile is non-uniform due to the intrinsic top-bottom asymmetry of 3-junction cells [4]. By breaking symmetry one can increase the flatness of the phase profile and increase the radiation power from the array. Further, for the systems with strongly broken symmetry this prominence of the profile can change its sign. One can break symmetry by changing the parameters of edge junctions, but in this case it is impossible to control it during the experiment. Therefore, it is more feasible to break symmetry by an adjustable parameter. As this parameter we choose the trim current [4].

In this report, we describe the design of the array with adjustable asymmetry and present first results of experiments performed on single-row triangular arrays with trim currents.

Chapter 2

Experiments

2.1 Junctions and array layout

According to our layout and specification, the samples were prepared at the foundry of the Institute for Physical High Technology (IPHT) in Jena, Germany. The size of each junction is about $9\mu\text{m}^2$. The cell size is about $S = 162\mu\text{m}^2$. The row consists of ten square cells. To the edge junctions we have connected two pairs of leads for trim currents and the voltage is measured from one pair of this leads. In previous experiments due to have a overdamped case, i.e. a small cell inductance, what is one of the main conditions to synchronize the system, we have measured at higher temperatures. In current circuit to have overdamped state at $T = 4.2\,K$ we have shunted each junction with a resistor. As an example of the geometry, in Fig. 1 we show a schematic view of a 6-cell array (a) with trim current leads and also a layout of the circuit.
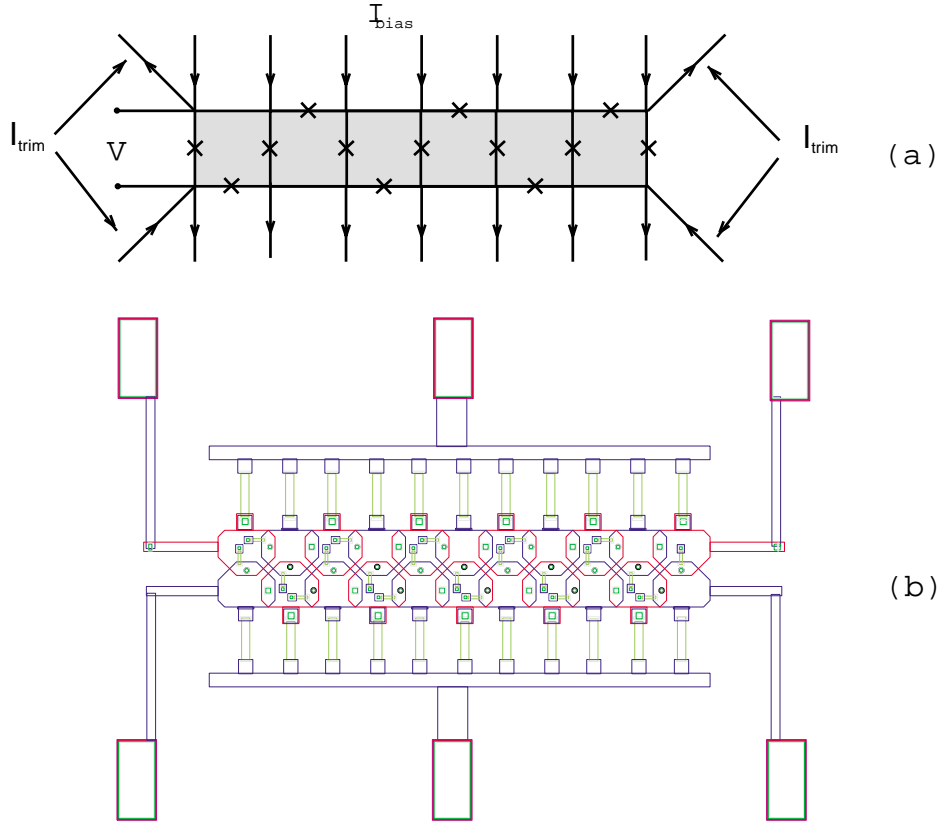

Figure 1: Schematic view (a) and layout (b) of the designed array of shunted Josephson junctions.

The external bias current (I_{bias}) is uniformly injected at each node of the array via $16\,\Omega$ resistors (along the vertical direction in Fig. 1b), and a voltage response (V) is measured across the vertical junctions. The junctions on the edges of the array are biased by trim current (I_{tr}) through additional leads. The discreteness of the array is expressed in terms of the parameter $\beta_{\text{L}} = 2\pi\frac{LI_c}{\Phi_0}$, where L is the self-inductance of the elementary cell, I_c is the critical current of the single junction, Φ_0 is the flux quantum. The inductance of the cell can be estimated as $L = 1.25\mu_0\sqrt{S}$. The damping of the junctions is defined in terms of the McCumber parameter, $\beta_{\text{C}} = 2\pi\frac{I_c R_{\text{S}}^2 C}{\Phi_0}$. Here R_S is the resistance and C is the junction capacitance. We estimate these parameters of our array to be $\beta_L \simeq 2$ and $\beta_C \simeq 1.8$ at $4.2\,K$.

2.2   Measurements

The dc measurements included the current-voltage (I-V) characteristics and $I_c(H)$ patterns of the array. All the results presented below were obtained at $T = 4.2\,K$.

Measurements were performed in the presence of a magnetic field perpendicular to the array plane, which controls the frustration through the array cells. In order to decrease external noise, we applied the dc bias through RC-filters with the cut-off frequency of about 1 MHz. The filters were mounted on the top of the dip-stick at room temperature. Residual dc magnetic field was screened by a cryoperm shield. The $I - V$ curve and $I_c(H)$ pattern at $I_{\text{tr}} = 0$ are shown in Fig. 2. One can note that this $I - V$ curve looks like overdamped. This is due to shunting of the junctions by shunt resistor of $R_s \simeq 6.5\Omega$. In Fig. 2b we show the critical current patterns versus magnetic field. The black curve shows the absolute value of the critical current I_c for Ibias > 0 and the red one shows the same for Ibias > 0. In the presence of frustration, we observed two resonant steps in the I-V curves of the array. The first step appears at the voltage of about 80-100 μV, the second one is at about 180-200 μV.

For suppling I_{bias} and I_{tr}, we used two independent battery-powered current sources. In order to check for the cross talk between the current sources at first we measured dc characteristics of the array with and without connecting the trim current source set to zero current. The characteristics of the array did not change upon connecting the idle I_{tr} source. Further we measured critical current dependence versus magnetic field at fixed values of the trim current. We measured these dependences in two directions of the bias current while trim current is kept constant. For Ibias > 0, the trim current and bias current flow in opposite directions (Fig. 3a), and for Ibias < 0 they have the same directions (Fig. 3b).

In Fig. 3 we present critical current patterns versus perpendicular magnetic field. First graph shows $I_c(H)$ corresponds to the opposite Ibias and Itr currents biasing. From these curves one can see that the counter flow of the trim current increases the critical current. In contrast the trim currents with same direction as the bias current decrease the critical current (Fig.4(b)). On both graphs we marked the frustration values for which we will present current-voltage characteristics in Fig. 4. This values of frustrations correspond either to the states at which resonant steps appear on $I - V$ curves, or to the states corresponding to the transition between the two resonant steps.

In Fig. 4 one can see $I - V$ curves of the array for various frustrations with current trimming. We show the curves for $f = -0.78$, $f = -0.47$, $f = 0.3$, $f = -0.41$, Fig. 4 from (a) to (d), respectively. According to numerical calculations and theory, [8, 8] at the checkerboard state the emitted radiation power reaches its maximum. This state is achieved at the half-integer frustration values. Fig. 4(b) and Fig. 4(d) correspond to frustrations near to one half and there are steps observed at 80-100 μV. first harmonics of the oscillations of the horizontal Josephson junctions. We note that the height of the step depends on the trim current. For small trim currents it grows and reaches its highest value at about $I_{\text{tr}} \simeq 30\,\mu A$. Further increasing of the trim current leads to a decrease in the step height. This effect can be explained by phase profile of the cells. As we noted in the Introduction, when the prominence of the profile is zero, i.e. when all phases are equal, the height of the step reaches
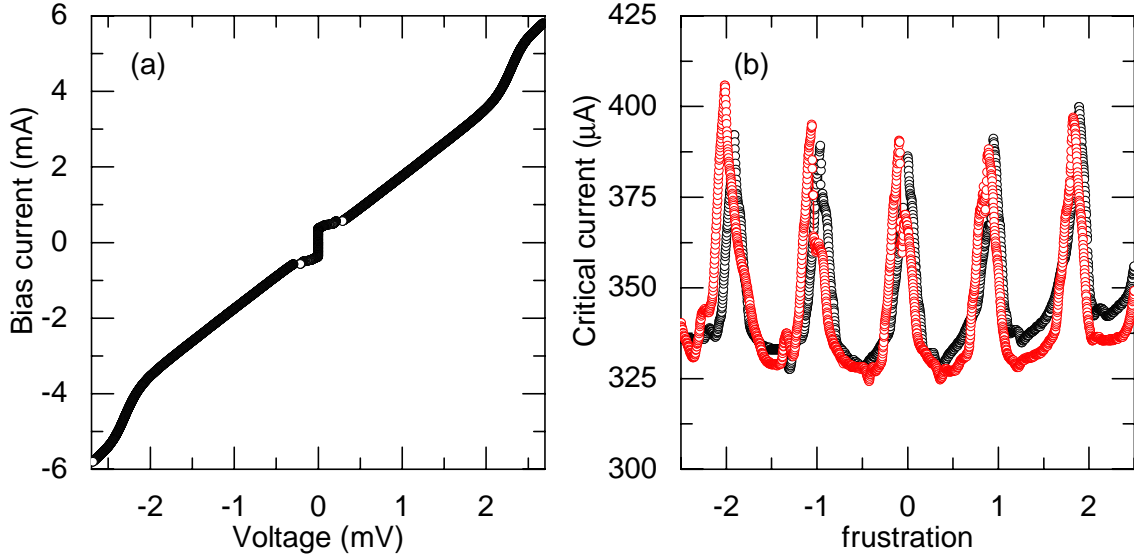
Figure 2: Dc characteristics of the array: (a) I-V curve; (b) $I_c(H)$, see text plus directions of the bias current, red one for opposite direction.
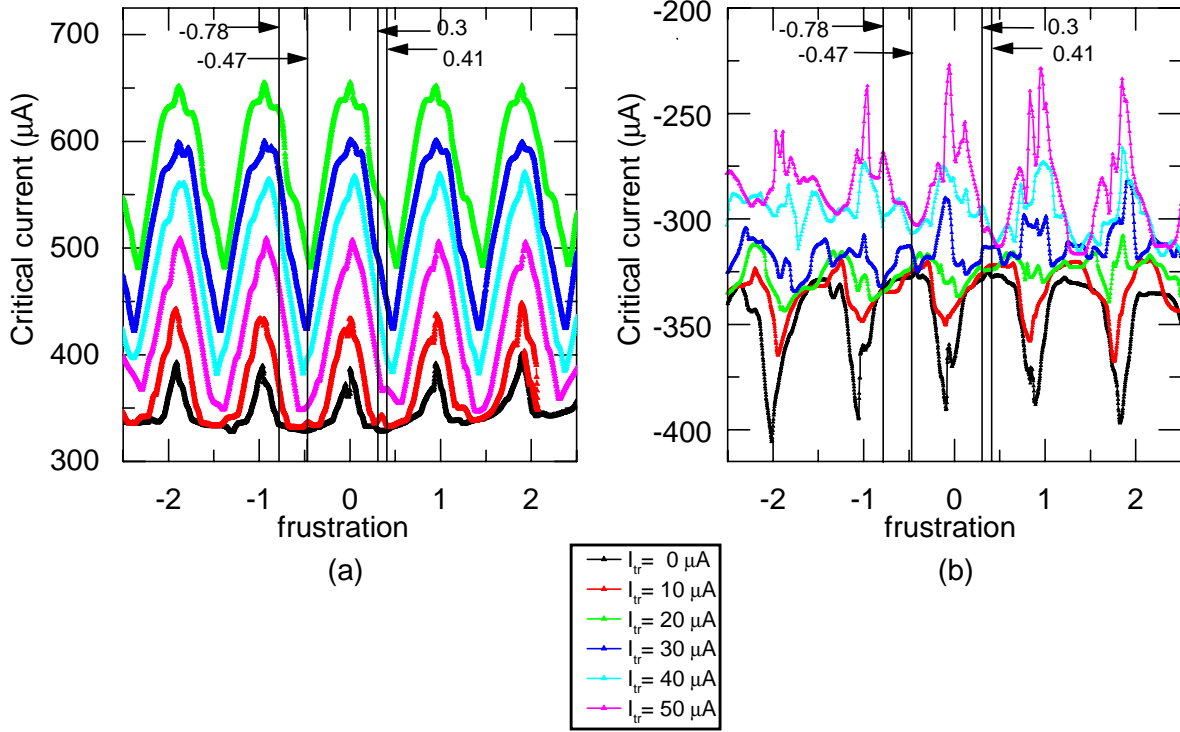

Figure 3: $I_c(H)$ pattern of the array for a set of trim currents. (a) and (b) show positive and negative critical currents, respectively.

its maximum. In Fig. 4(a) we present the $I - V$ curves for frustration -0.78. For this value of the frustration there exists a step at voltage 180-200 μV which corresponds to the second resonance. The height of this step also displays clear dependence on the trim current I_{tr}, and it is most pronounced at $I_{tr} \simeq 30 \, \mu A$. Fig. 4(c) shows the $I - V$ curves for the intermediate state between the above the two cases, showing both the first and second steps.
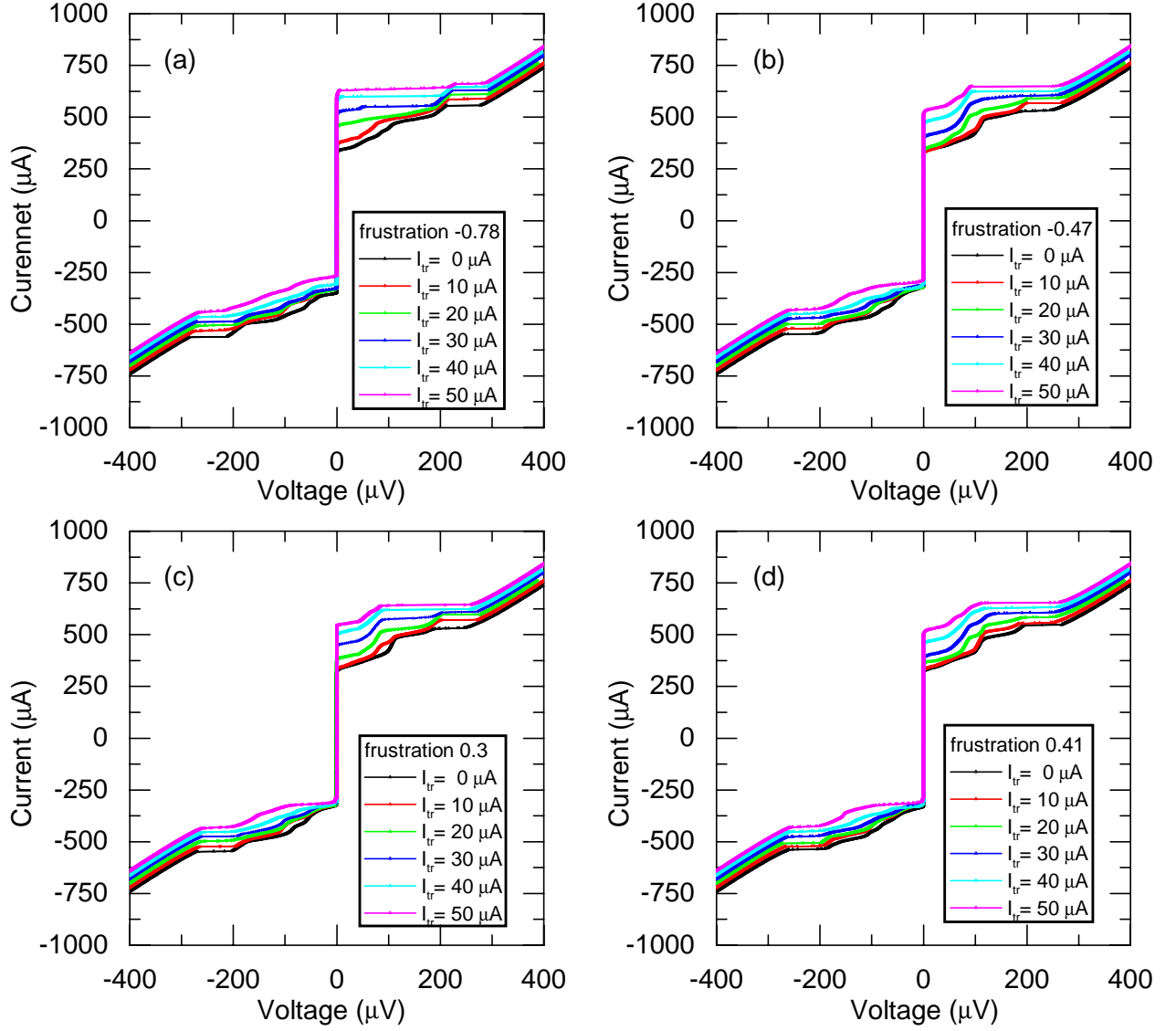
6

Figure 4: *I-V* curves of the array for a set of trim currents at various frustrations, (a) $f = -0.78$, (b) $f = -0.47$, (c) $f = -0.3$, (d) $f = -0.41$,

Conclusions

We reported experimental observation for the effect of trim current on triangular arrays of shunted Josephson junctions in a perpendicular magnetic field. The resonant steps enhancement due to breaking of the symmetry of the array by trim current was observed. This is consisted with the expectation that trim currents may increase flatness of the phases profile. We suppose that trim current may help to stabilize coherent oscillations and increase the operation margins and emitting radiation power. Still, the array response on trim currents is rather complicated. More dc measurements should be done to fully justify feasibility of using trim currents in more complex designs with rf-power coupled out of the array.

Bibliography

[1] S.Y. Han, B.K. Bi, W.X. Zhang and J.E. Lukens, demonstration of Josephson effect submillimeter-wave sources with increased power, Appl. Phys. Lett. **64**, pp.1424-1426 (1994)

[2] S.P. Yukon and N.C.H. Lin, Generation of mode locked pulses using 2D triangular Josephson junction arrays, IEEE Trans. Appl. Supercond., **7**, No.2, pp.3115-3121 (1997)

[3] S.P. Yukon and N.C.H. Lin, Josephson junction phased arrays, IEEE Trans. Appl. Supercond., **9**, No.2, pp.4533-4537 (1999)

[4] S.P. Yukon and N.C.H. Lin, Maximizing microwave power from triangular Josephson junction arrays, IEEE Trans. Appl. Supercond., **9**, No.2, pp.4320-4324 (1999)

[5] P. Caputo, A.V. Ustinov, N.C.H. Lin and S.P. Yukon, Radiation from triangular arrays of Josephson junctions. IEEE Trans. Appl. Supercond., **9**, No.2, pp.4538-4541 (1999)

[6] P. Caputo, A. Duwel, T. P. Orlando, A. V. Ustinov, N. C. H. Lin, S. P. Yukon, Experiment with triangular Arrays of Josephson Junctions, in Proc. of Eur. Conf. on Applied Superconductivity, Eds. H. Koch and S. Knappe, (Publisher: Physikalisch-Technische Bundesanstalt, Braunschweig, 1997), pp. 180-182.

[7] P. Caputo and A. V. Ustinov, Final Report on Analysis of Triangular Arrays of Josephson Tunnel Junctions, contract F61775-98-WE041, May 1999.

[8] S.P. Yukon and N.C.H. Lin, Dynamics of triangular and tetrahedral Josephson junction oscillator arrays, IEEE Trans. Appl. Supercond., **5**, No.2, pp.2959-2964 (1995)

Testing of Josephson array antennas and trim currents tuning[*]

A.A. Abdumalikov, D. Abraimov and A. V. Ustinov

Physikalisches Institut III, Universität Erlangen-Nürnberg
D-91054 Erlangen, Germany

March 2001

Contents

Abstract

This interim report presents new results obtained to date for the two sub-projects of the planned research. The first one deals with LTLSM (Low Temperature Laser Scanning Microscope) detection of a distribution of radiation power over a chip containing a Josephson oscillator. The second group of results focus on further measurements of arrays with trim currents. We observed that trimming changes the shape and position of the resonant step and creates new steps at lower voltages. We have measured detailed dc-characteristics of the square cell triangular arrays with five and ten cells in the presence of perpendicular magnetic field.

1 Low Temperature Laser Scanning Microscopy (LTLSM)

1.1 LTLSM principle and setup

The LTLSM method [1, 2, 3, 4, 5, 6] is based on recording an electrical response of the sample as a function of a local action of the laser irradiation. The electrical response occurs mainly due to local temperature change in the laser-illuminated spot and, thus, depends on the coordinates of the laser spot on the sample surface. The response can be visually represented as a two-dimensional image reflecting thermally-sensitive parts of the circuit. In order to improve the signal-to noise ratio and to increase spatial resolution, the beam intensity is modulated at a frequency of several kHz and the circuit response is detected using lock-in technique. The most standard way is to bias some active circuit of the device at a constant current and register a voltage drop measured on various terminals on the device.

We intend to use the method of LTLSM in our studies of mutually coupled arrays of Josephson junctions. LTLSM measurements of spatially-distributed radiation power of array oscillators over their coupling circuits passive lines, etc. required an on-chip radiation detector to be integrated at stage of chip design. As a starting point, we have chosen to test the developed on-chip detection circuitry with a well known characterized oscillator. As such an oscillator we have chosen a wide annular Josephson junction (WAJJ) featured with a strip line coupler.

We biased a wide annular Josephson junction at a certain current I_{WAJJ} setting its radiation frequency $f_{\mathrm{WAJJ}} = V_{\mathrm{WAJJ}}/\Phi_0$. During these measurements we kept the bias current I_{WAJJ} constant. We used two different outputs to measure the spatially-dependent voltage response. In type I measurements, we were detecting voltage change $\delta V_{\mathrm{WAJJ}}(x_l, y_l)$ on WAJJ itself as a function of the laser beam position. In type II measurement, we were using small SIS double-junction as a detector of radiation emitted by WAJJ. It was done by measuring $\delta V_{\mathrm{SIS}}(x_l, y_l)$ in the current bias mode. In both cases, the laser beam has been scanned in the area of the annular junction.

For measurements, a chip was glued on a liquid helium-cooled copper sample holder placed in vacuum near an optical cryostat window. The optical system of the scanning microscope [5] focused the beam of a 2 mW He-Ne laser into a spot of about 2 μm in diameter on the chip. The beam was deflected within 0.25 mm × 0.25 mm field by an electromagnetic mirror scanner controlled by a computer. The entire optical system could be shifted with 0.5 μm step increments parallel to the sample plane by computer-controlled step motors within 5 mm × 5 mm field. Our setup permits also obtaining photo images of the investigated structure by measurement of the intensity of the reflected light versus laser beam coordinates (see Fig. 2(a)). For a precise temperature adjustment we inserted a thermal sensor and bifilar

heater into the sample holder and controlled the precise temperature using an electronic PID regulator.

1.2 Radiation from WAJJ and on-chip rf coupling circuitry

A vortex steadily moving in an annular Josephson junction at velocity u driven bias current γ generates a voltage $V \propto u$ across the junction. As it was shown recently [7] vortex moving in *wide* annular Josephson junction at some particular angular frequency comes into resonance with a whispering gallery mode electromagnetic excitation. This phenomenon results in a fine structure on the current-voltage characteristics of the WAJJ. In such a case the same Josephson vortex is used for both exciting and detecting the whispering gallery mode. It is rather interesting to obtain electromagnetic wave power profile corresponding to whispering gallery mode in WAJJ. Our earlier experiments by LTLSM technique show, that detecting voltage change $\delta V_{\mathrm{WAJJ}}(x_l, y_l)$ on WAJJ itself lacks the sensitivity to do that. In this way LTLSM images corresponding to different modes were found undistinguishable.

The radiation associated with the time-dependent fields emitted from WAJJ can be measured on-chip directly. The concept of on-chip detecting circuit [8, 9, 11, 10] had been implemented for such purpose.
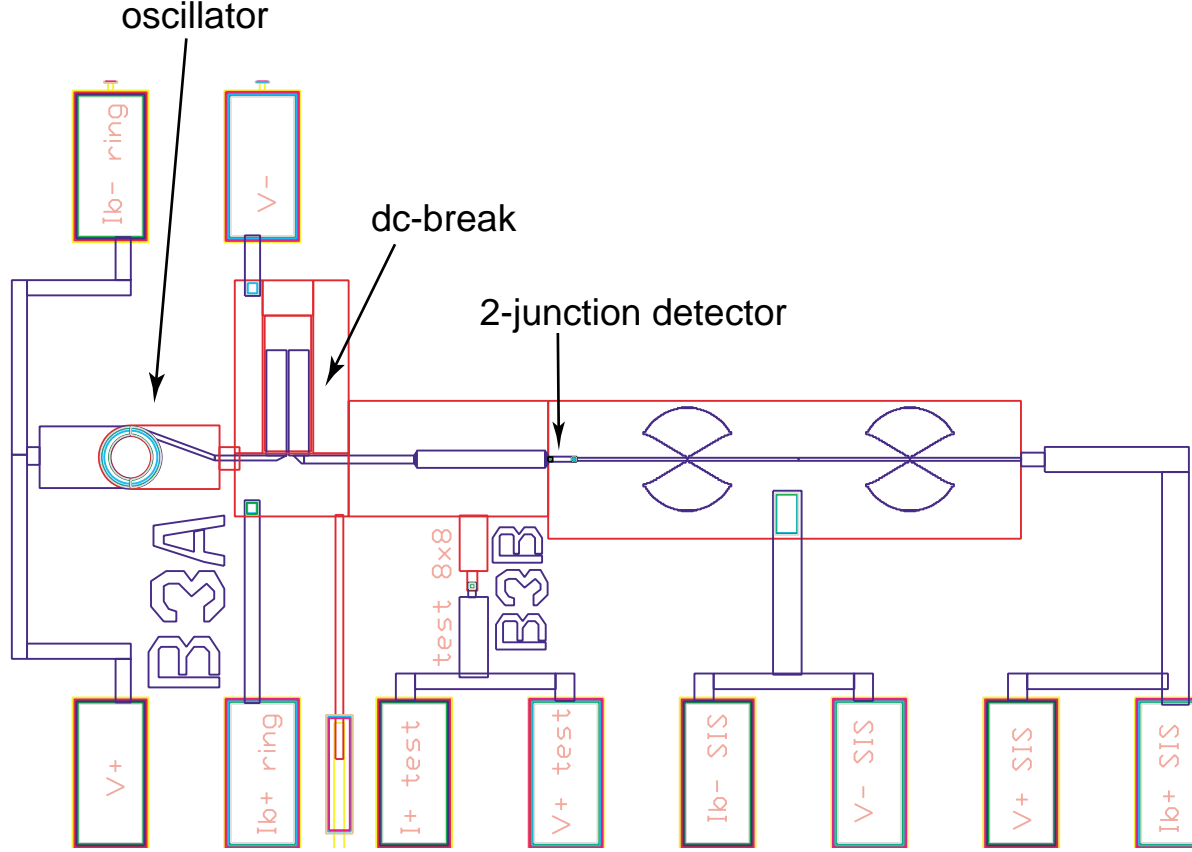

Figure 1: Layout of the coupling circuit and detector.

The samples according to our design and specification were prepared at the foundry of the Institute for Physical High Technology (IPHT) in Jena, Germany [12]. A layout of the circuits used to couple the radiation out from the wide annular Josephson junction to a SIS

detector is sketched in Fig. 1. The radiation from the WAJJ passes by transmission line to SIS detector. To decouple detecting and emitting junctions galvanically, a dc-break had been used. To prevent leak of radiation from SIS detector, rf stub filters had been added. Both symmetrical and non-symmetrical transmission line connections to the WAJJ have been used.

1.3   Measurement results

It is known [13] that for the hot-spot methods the voltage response from a Josephson tunnel junction biased at gap regime corresponds to distribution of the energy gap $\Delta(x, y)$ over the junction area. To verify homogeneity of WAJJs voltage responses $\delta V_{\mathrm{WAJJ}}(x_l, y_l)$ at voltage $V_{\mathrm{WAJJ}} = 1.8mV$ has been scanned. In the Fig. 2(b) white areas correspond to negative voltage response. The LTLSM images from different measured WAJJ show that in the connection with transmission line coupler induces no inhomogeneity of the gap voltage.
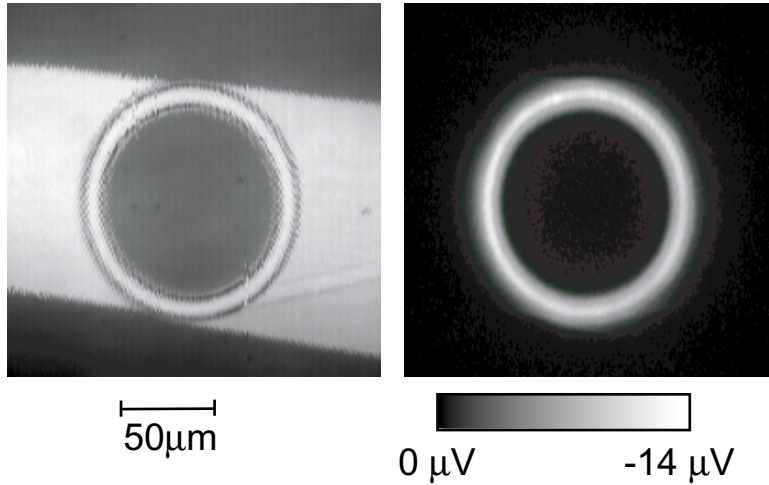

Figure 2: (a) Optical image of WAJJ obtained using the reflected light in situ of LTLSM setup. (b) δV_{WAJJ} response of the WAJJ biased at gap regime .

Vortices in WAJJ were trapped by applying a small bias current during cooling down from the normal to the superconducting state. Vortex states are identified as the quantized voltage step observed on the current-voltage characteristics. In Fig. 3(b) the single-vortex characteristic of the junction from B3A circuit is presented. Unfortunately, from the residual pinning current we have to admit that rather large amount of parasitic magnetic flux remains trapped during this measurement in the WAJJ electrodes.

Typical $I - V$ characteristics of the SIS detector measured with and without WAJJ pumping for the same sample are plotted in Fig. 3(a). The critical current of SIS detector is suppressed in the presence of radiation a photon assisted tunneling step appears in the sub-gap region of the I-V curve. The SIS voltage response δV_{SIS} measured at a constant SIS current (red bias point in Fig. 3(a)) and constant WAJJ current is shown in Fig. 4(a). For comparison, Fig. 4(b) presents a response δV_{WAJJ} measured for the same junction.
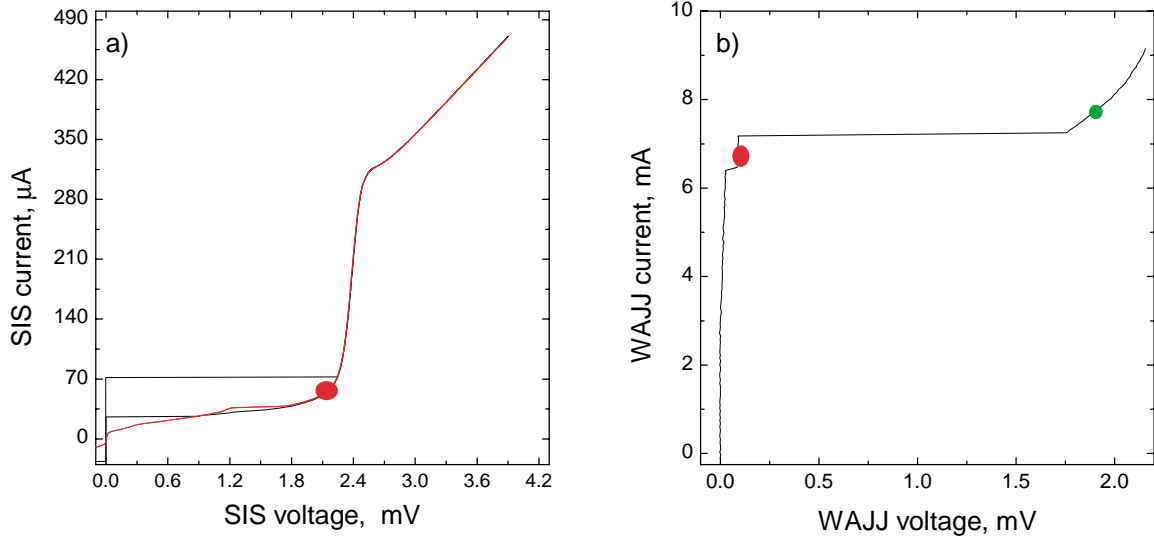
Figure 3: (a) $I - V$ characteristics of the SIS detector measured with and without WAJJ pumping , (b) $I - V$ characteristic of the WAJJ, the red marks indicate bias points for LTLSM measurement, the green circle indicates the bias point for testing WAJJ homogeneity (Fig. 2(b)).
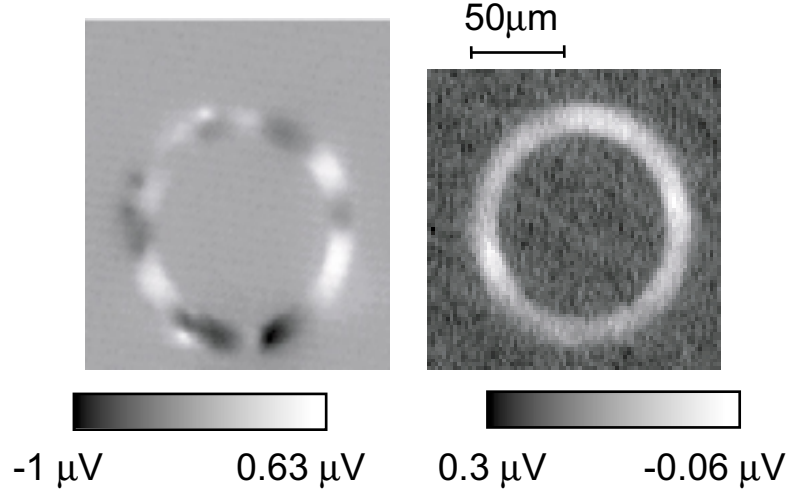

Figure 4: (a) δV_{SIS} LTLSM response of the WAJJ (sample B3A) biased at 3-fluxon step ($V_{\mathrm{SIS}} = 1.82\ mV$, $I_{\mathrm{SIS}} = 55.77\ \mu A$, $V_{\mathrm{WAJJ}} = 225\ \mu V$), (b) δV_{WAJJ} response at 1-fluxon step ($I_{\mathrm{WAJJ}} = 108\ \mu A$, $V_{\mathrm{WAJJ}} = 50\ \mu V$).

2 Trim current tuning

2.1 Measurements

Here we report our further experimental results with current trimming in triangular arrays. We have systematically measured two more samples. According to our layout and specification, the samples were prepared at the foundry of the Institute for Physical High Technology (IPHT) in Jena, Germany. The first sample has 10 cells while the second has

only 5 cells. Except the cell number, all other geometrical parameters of the samples are same. The size of each junction is about $9\,\mu m^2$, the cell size is about $162\,\mu m^2$. To simulate the high temperature superconductors and to have overdamped junctions, we have shunted all the junctions with the resistance of about 6.5Ω. To the edges of both samples we have connected two pairs of leads for trim currents. The voltage is always measured across one pair of this leads. All of the measurements were performed in liquid helium ($T = 4.2\,K$).

We measured the dc characteristics of the samples. The dc measurements included the current-voltage ($I - V$) characteristics and $I_c(H)$ pattern. We also measured step voltage dependence on the field ($V_{\mathrm{step}}(H)$). Details about measurement setup can be found in our previous report [14]

We note by $I_{\mathrm{bias}} > 0$ that the trim current and bias currents flow in opposite directions and by $I_{\mathrm{bias}} < 0$ the case when they have the same directions.
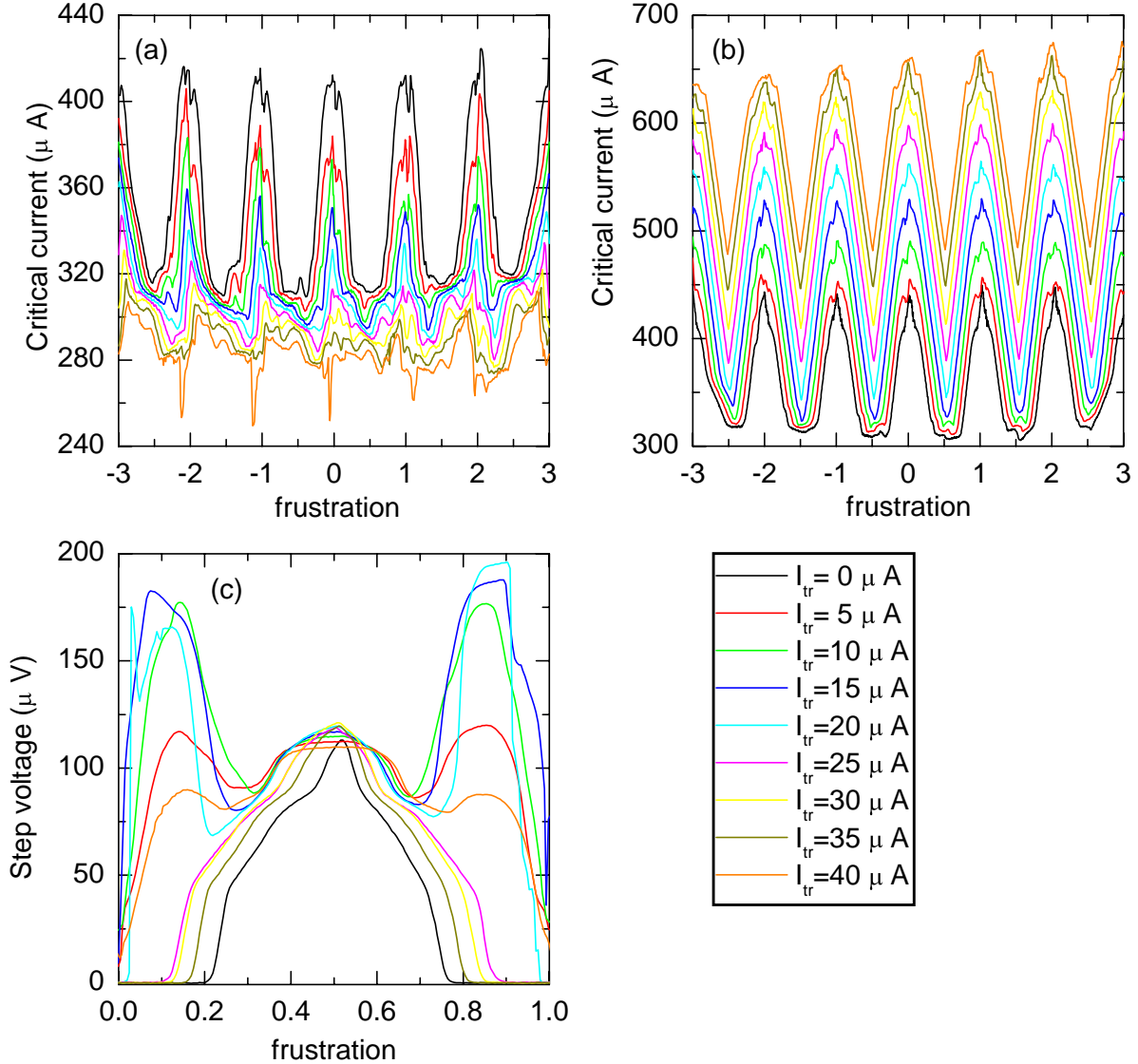

Figure 5: Perpendicular magnetic field depend dc characteristics of the 10 cell array: (a) $I_c(H)$ pattern for $I_{\mathrm{bias}} < 0$, (b) $I_c(H)$ pattern for $I_{\mathrm{bias}} > 0$, (d) $V_{\mathrm{step}}(H)$ for $I_{\mathrm{bias}} \approx 510\,\mu A$.

In the Fig. 5 and Fig. 6 we present dc characteristics which depend on perpendicular

magnetic field for ten-cell and five-cell arrays, correspondingly. Each of these figures $I_c(H)$ patterns, (a) and (b), and step voltage dependence on frustration (c). From these figures one can see, that increasing the trim current changes the $I_c(H)$ pattern such that the critical current increases for the counter flowing of the trim current and decreases for the same directions of the currents.
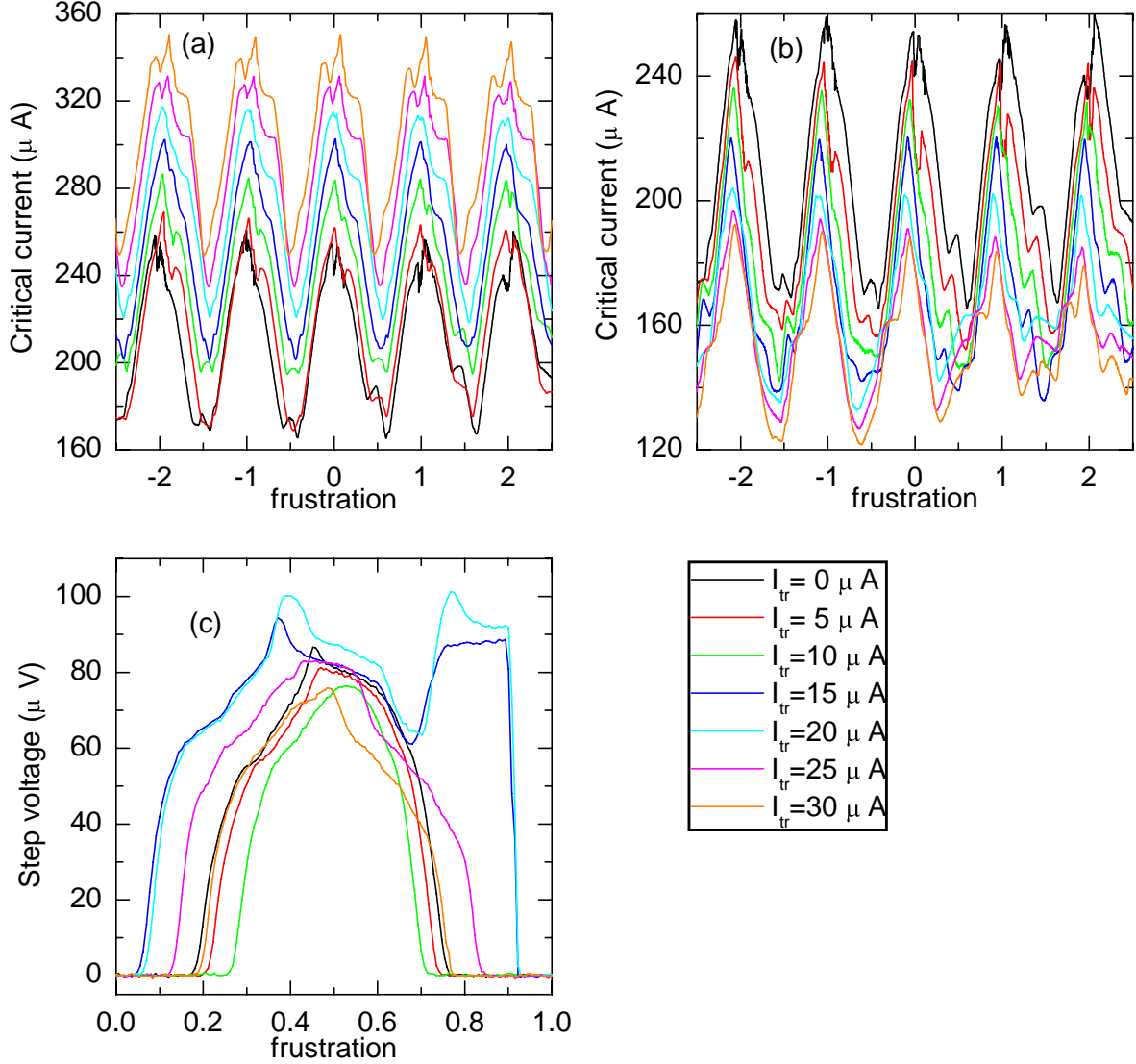

Figure 6: Perpendicular magnetic field depend dc characteristics of the 5 cell array: (a) $I_c(H)$ pattern for $I_{bias} < 0$, (b) $I_c(H)$ pattern for $I_{bias} > 0$, (d) $V_{step}(H)$ for $I_{bias} \approx 250\,\mu\text{A}$.

As it was mentioned in our previous report [14], according to numerical calculations and theory [15], at the checkerboard state the emitted radiation power reaches its maximum. This state is achieved at the half-integer frustration values. In Fig. 7 are shown $I - V$ curves of the array with 10 cells, for two values of the frustration, zero (Fig. 7(a)) and one half (Fig. 7(b)). Figure for $f = 0.5$ shows the major resonant step predicted by theory. From these curves we note that the current trimming changes the height of the resonance at 100-120 μV and creates an other step at lower voltages (70-90 μV) which grows with trim current. For trim current larger then 40 μA the height of this step decreases and at $I_{tr} = 40\mu A$ there appears

7

still another step at even lower voltages ($\approx 50\mu$V), but only for $I_{\text{bias}} > 0$. The step voltage dependence on frustration is shown for several values of trim current in Fig. 5(c). These curves were measured for $I_{\text{bias}} \approx 510\,\mu$A at which the step at voltage $\approx 120\mu V$ at frustration one half.
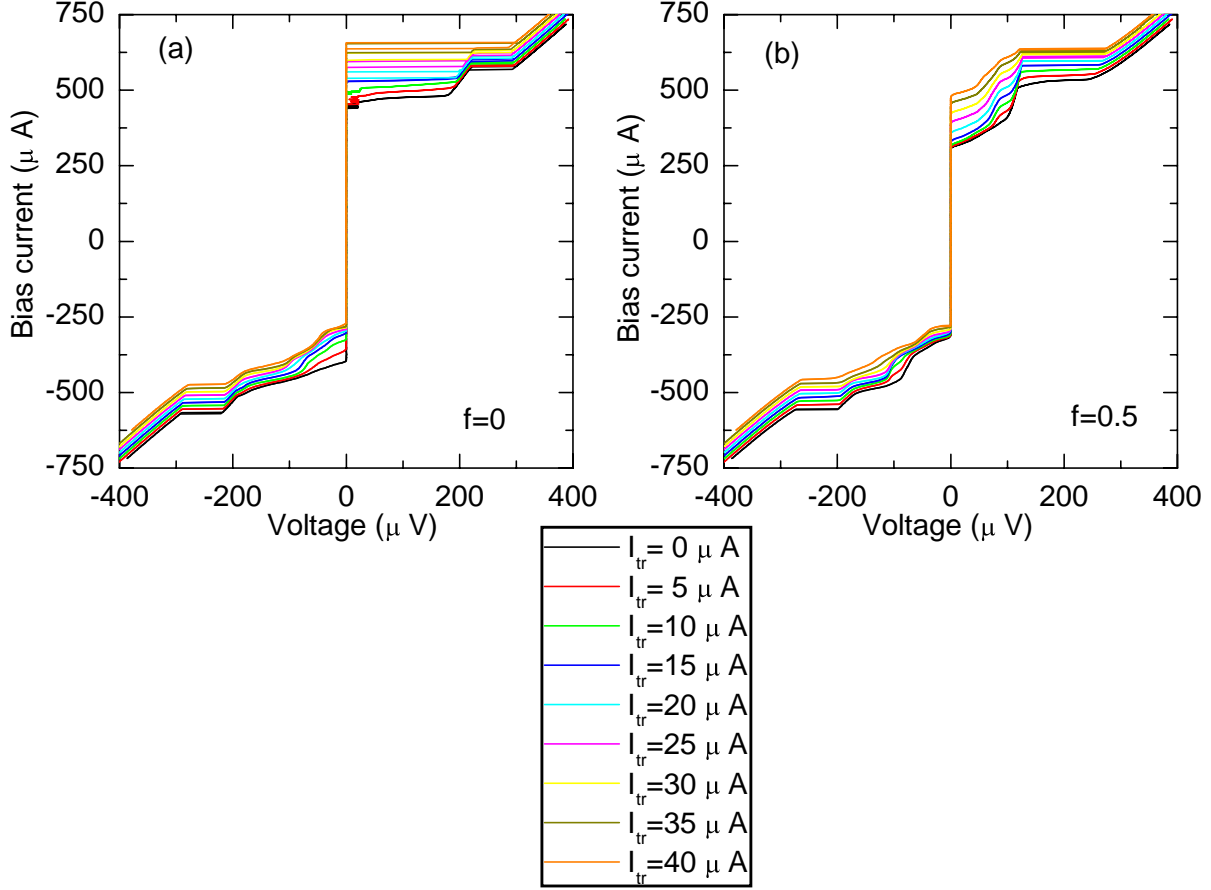

Figure 7: $I - V$ curves of the array with ten cells for a set of trim current values at zero frustration (a) and at frustration one half (b).

The $I - V$ curves of the array with 5 cells are shown in Fig. 8. The Fig. 8(a) corresponds to $f = 0$ and the Fig. 8(b) to $f = 0.52$. For this array, also we observed resonances but at lower voltages (60-80 μV). The current trimming changes the shape of the step and shifts its position to lower voltages. In Fig. 8(c) we present the enlarged $I - V$ curves around the step for $I_{\text{bias}} > 0$. At $I_{\text{tr}} = 30\mu A$ we observed small back bending of the resonance step. This may occur due to the amplitude-dependent correction to the resonance frequency [16]. It may occur because of large amplitude of the oscillations of horizontal junctions. In perturbation theory for the system one should take into account non-linear terms which give negative frequency shift. In Fig. 6(c) we show the step voltage dependence on external perpendicular magnetic field. Such dependences were also measured for most of sharp steps at half frustration (can be provided on request).
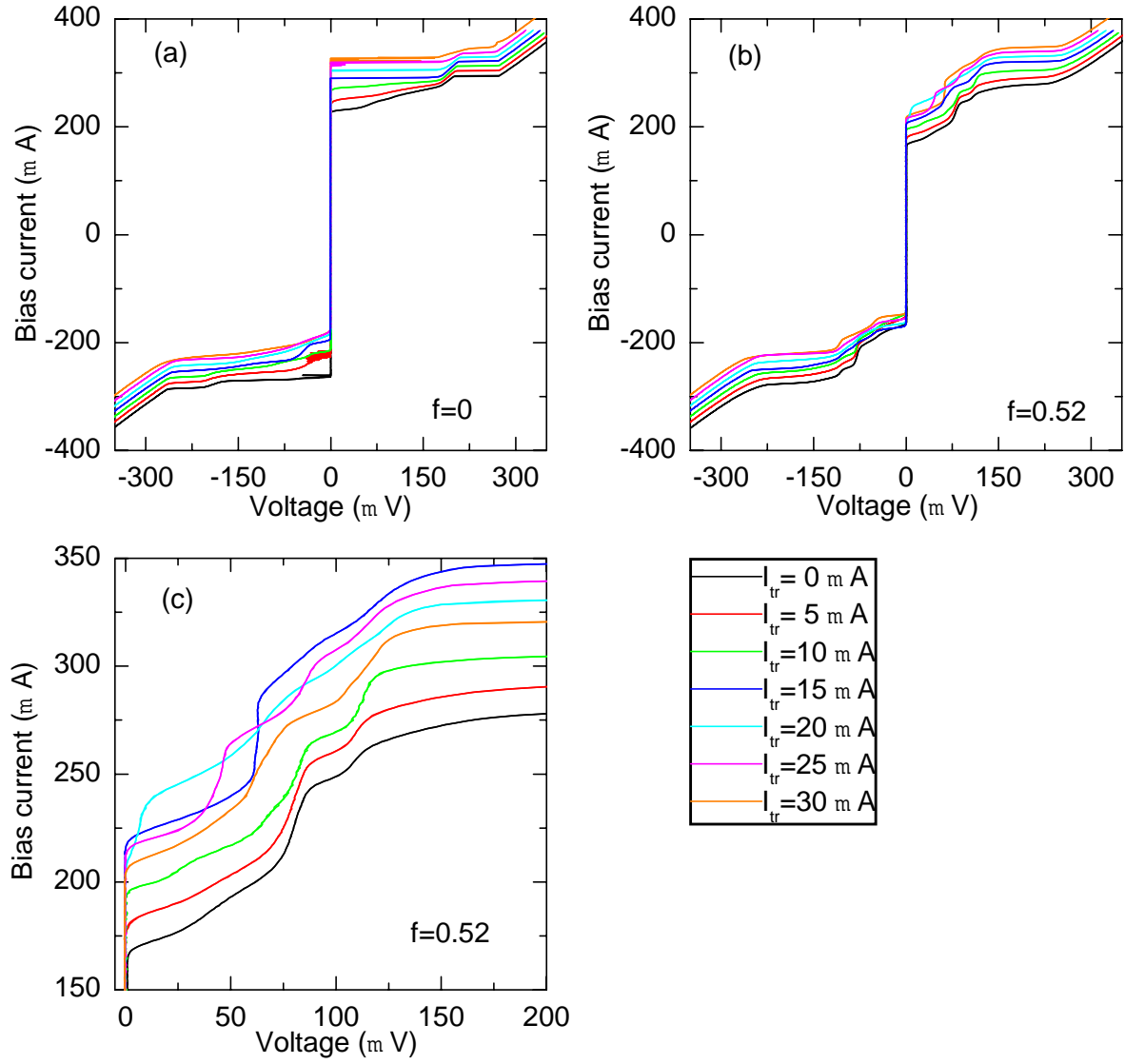
8

Figure 8: $I - V$ curves of the array with five cells for a set of trim current values at zero frustration (a) and at $f = 0.52$ (b).

3 Discussion

We reported here our first LTLSM measurements using an on-chip radiation detection scheme. Radiation emitted by annular wide Josephson tunnel junction was visualized. The used technique allowed to visualize the interference pattern of the standing electromagnetic waves in WAJJ at V_{WAAJ} voltage corresponding to the single-fluxon state. The $\delta V_{SIS}(x_l, y_l)$ response is found to be very similar to the pattern of the $\delta V_{WAJJ}(x_l, y_l)$ response. Absolute value of the response signal from SIS detector is at least two times larger than the voltage response from WAJJ. In case of the δV_{SIS}-type measurements signal-to-noise ratio is ~ 5.7 times better than for the δV_{WAJJ}-type measurements. The capability of the laser scanning technique of monitoring Josephson junctions dynamics, verifying new designs of cryoelectronic sub-millimeter circuits, and testing the chip quality is demonstrated in these measurements.

We have experimentally investigated the dynamics of triangular arrays of shunted Joseph-

son junctions in perpendicular magnetic field, with currents trimming. We have systematically measured dc characteristics of two arrays with 5 and 10 cells. The resonant steps change their shape due to breaking symmetry of the system. For the five cell array we observed backbending of resonance step at larger trim currents. Due to current trimming there appear steps at lower voltages. Precise understanding of the nature of the observed steps and of the expected profile of ac voltages along the arrays requires detailed numerical simulations with specific parameters of our experiment.

References

[1] C. C. Chi, M. M. T. Loy, and D. C. Cronemeyer, Appl. Phys. Lett. **40**(5) 437 (1982)

[2] M. Scheuermann, James R. Lhota, P.K.Kuo, and J. T. Chen, Phys. Rev. Lett. **50**, 74 (1983)

[3] V. A. Konovodchenko, A. G. Sivakov, A. P. Zhuravel', V. G. Efremenko, and B. B. Banduryan, Sov. J. Low Temp. Phys. **12**, 311 (1986)

[4] Yu. Ya. Divin, F. Ya. Nad', V. Ya. Pokrovski, P. M. Shadrin, IEEE Transactions on Magnetics, **27**, No.2, 1101 (1991)

[5] A. G. Sivakov, A. P. Zhuravel', O. G. Turutanov, I. M. Dmitrenko, Appl. Surf. Sci. **106**, 390 (1996)

[6] James C. Culbertson, Harvey S. Newman, Charles Wilker, J. Appl. Phys. **84**, N. 5, 2768 (1998)

[7] A. Wallraff, A. V. Ustinov, V. V. Kurin, I. A. Shereshevsky, and N. K. Vdovicheva, Phys. Rev. Lett. **84**, 151 (2000)

[8] T. Nagatsuma, K. Enpuku, K. Yoshida, and F. Irie, J. Appl. Phys. **56** (11) 3284 (1984)

[9] S. V. Shitov, A. V. Ustinov, N. Iosad, and H. Kohlstedt, J. Appl. Phys. **80** (12) 7134 (1996)

[10] A. A. Abdumalikov, P. Caputo and A. V. Ustinov, Interim Report No.1 on Experiments with mutually coupled arrays of Josephson junctions, contract F61775-00-WE004, September 2000

[11] V.P. Koshelets and S.V. Shitov, Topical review: Integrated superconducting receivers, Supercond. Sci.Technol. **13** R53-R69. (2000)

[12] http://www.ipht-jena.de/

[13] R.Gross, M. Kyanagi, H. Seifert and R. P. Huebener, Phys. Lett. **109A** 298 (1985)

[14] A.A. Abdumalikov P. Caputo, A. V. Ustinov, Interim Report No.1 on Testing of Josephson array antennas and trim currents tuning, contract F61775-00-C0004, September 2000.

[15] S.P. Yukon and N.C.H. Lin, Dynamics of triangular and tetrahedral Josephson junction oscillator arrays, IEEE Trans. Appl. Supercond., **5**, No.2, pp.2959-2964 (1995)

[16] A.V. Ustinov, B.A. Malomed, and E. Goldobin, A backbending current-voltage characteristic for an annular Josephson junction in magnetic field, Phys. Rev. B **60**, 1365, 1999

Final Report (No.3)

Testing of Josephson array antennas and trim currents tuning[*]

A.A. Abdumalikov and A. V. Ustinov

Physikalisches Institut III, Universität Erlangen-Nürnberg
D-91054 Erlangen, Germany

November 2002

Contents

Abstract

Here we report about our finally successful spatially resolved investigations of a series-parallel array (SPA). Measurements have been performed at different temperatures using low temperature laser scanning microscope (LTLSM). We have observed that the array response at the resonance branches is strikingly similar to that of a long Josephson junction in the flux-flow mode [1, 2].

1 Introduction

Various types of Josephson tunnel junction circuits are promising microwave radiation sources in mm and sub-mm wave range. Josephson junction arrays have been investigated extensively [3, 4]. However, the experimental studies of arrays were mainly restricted to the integral properties such as the I-V curve and the emitted high-frequency radiation. Spatially resolved investigations using laser beam scanning allow us to study here local properties as well as spatial patterns of the dynamical states in the arrays.

We have reported earlier about dc and ac measurement of a series-parallel arrays (SPA) in presence of an external magnetic field perpendicular to the substrate plane [5]. It was observed that the current-voltage characteristics of SPA has two resonances. We also have detected rather large radiation power at both resonances. It was surprising that measured radiation for resistive branch at higher temperature was larger then that of the second resonance at lower temperatures. In this report we present spatially resolved studies of SPA, which shed light on the dynamics of the resonant states.

2 Setup and technique

In the following we give a brief description of the experimental setup technique; for details we refer to our Interim Report No.2 [6]. The LTLSM setup consist of two parts: scanning laser microscope and liquid helium cryostat with optical window. The samples are fixed on a copper plate (which is in vacuum and has thermal contact to liquid helium) with a glue of high thermal conductance. The sample surface can be scanned with laser beam which passes through optical window of the cryostat. An external perpendicular magnetic field can be applied using a superconducting coil mounted in the helium bath. The whole sample holder is screened with a double cryoperm shield that reduces the effect of the external magnetic fields.

The main effect of the laser beam is a local heating of the sample around the beam position (x,y). The local temperature rises here by about 0.2 K. The spatial resolution of LTLSM about 1.5 μm. It is determined by the beam size and thermal healing length η in the sample. The scanning area of the microscope is 5x0.25 mm^2.

During the experiment we current bias the junction with a battery-powered current source. The laser beam causes a voltage change $\delta V(x, y)$ on the sample which is detected with a lock-in amplifier at laser power modulation frequency of about 2 kHz. While scanning over the sample the beam-induced voltage change is recorded by a computer. The response can be visually represented as a two-dimensional image reflecting thermally-sensitive parts of the current biased circuit.

3 Experiment

Using the reflected light in LTLSM setup we have obtained an optical image of the SPA presented in Fig. 1(a). It is known that for the hot spot methods the voltage response of a Josephson tunnel junction biased at or slightly below the superconducting energy gap corresponds to distribution of this gap $\Delta(x,y)$ over the junction area. To verify homogeneity of SPA junctions, the voltage response $\delta V(x,y)$ has been imaged at 2.3 mV. In Fig. 1(b) white dots correspond to voltage response. This LTLSM image shows that the junction properties over the whole array are very uniform.
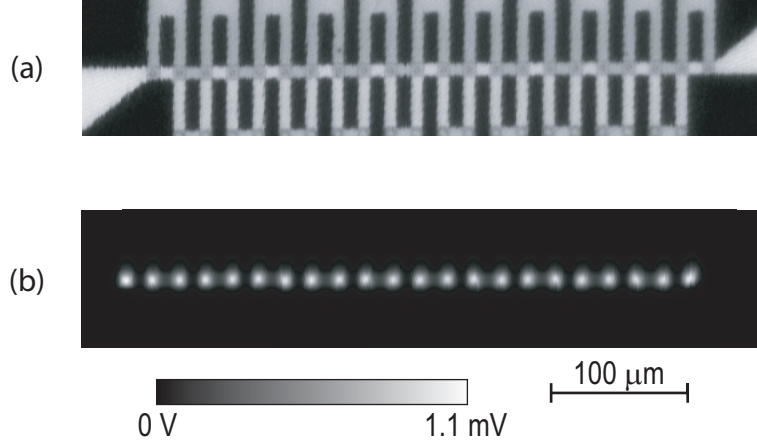

Figure 1: (a) Optical image and (b) $\delta V(x,y)$ response of SPA biased at the gap voltage. Temperature T=4.56 K.

During the experiment described below, the junctions were operated at the temperature T=7.5-8 K. The current-voltage characteristics of the investigated array at temperatures 7.71 K and 7.84 K are presented in Fig. 2. The I-V curves were measured at half frustrations corresponding to the local minimum of the critical current vs. frustration patterns presented in Fig. 3.
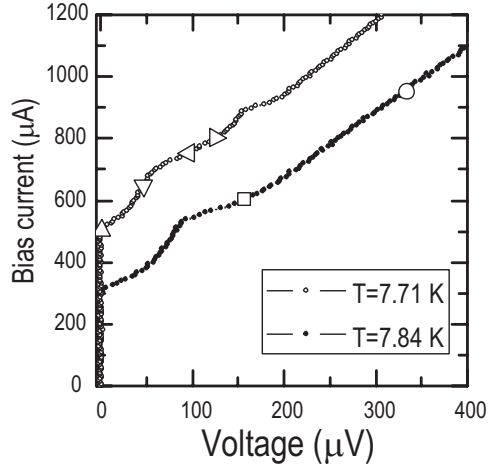

Figure 2: Current voltage characteristics of the investigated array at temperatures 7.71 K (small open circles) and 7.84 K (small solid circles). Larger symbols correspond to bias points of LTLSM images discussed below.

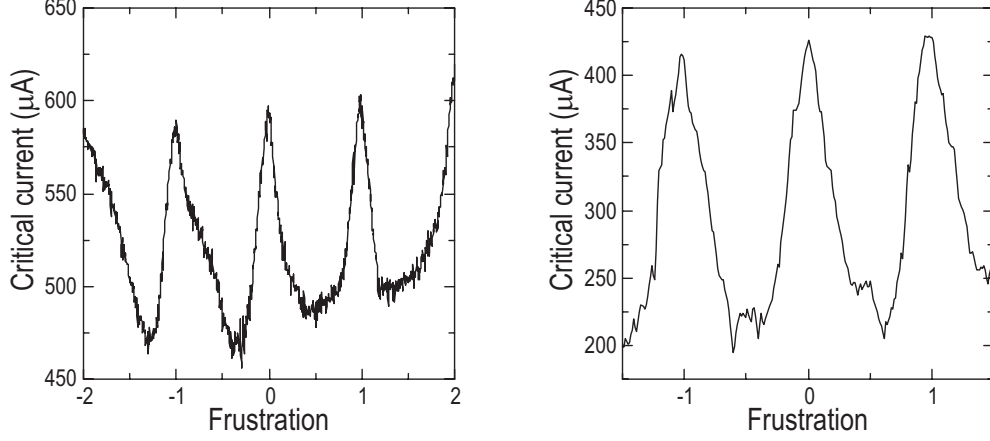On the I-V curve at 7.71 K we see two resonant branches. First resonance is at the voltage

Figure 3: Critical current vs. frustration patterns at (a) T=7.71 K and (b) T=7.84 K

of about 60 μV and the second is at the voltage of about 160 μV. The experimental laser-scanning data obtained at 7.71 K can be divided in to two groups: The imaged bias points are either on the first or on the second resonance branches.

We start from discussion of the data obtained at the first resonance. Figure 4 shows some of the imaging results. The images are represented by line-scan along the array and 2D scans. The line scans were obtained from the corresponding 2D scans by taking response for a fixed $y-$coordinate. The vertical axis (gray scale in 2D scans) displays the detected voltage signal δV(x) (or δV(x,y) in 2D scans). The scan in Fig. 4(a) was taken at the bottom of the resonance branch at the bias current I_{bias} =500 μA (up triangle in Fig. 2). The line scan shows that the response is observed only at the left border of the array and rapidly decays; the decay length is about 5 array cells ($\sim$ 80 μm). At the top of the first resonance (down

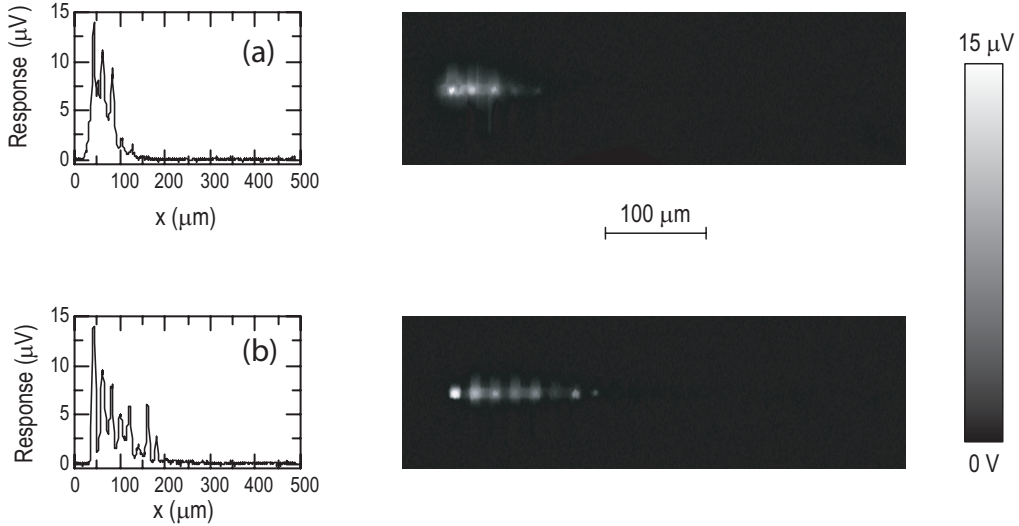Figure 4: LTLSM voltage response of the SPA at the first resonance for bias current (a) 500 μA and (b) 610 μA

triangle in Fig. 2, I_{bias} =610 μA) the decay length is longer, about 8 array cells ($\sim$ 140 μm). These results are similar to the behavior of a long Josephson tunnel junctions in a flux-flow regime [1, 2]. The interpretation of this effect in the case of long junction is that an increase of losses at the junction boundary due to the laser beam locally reduces fluxon velocity which results on the reduction of the voltage across the array. The fluxons enter the array from left

4

end where they are still slow and a small change of the dissipation leads to the large change of their velocity.

For the second resonance, the laser scanning data are drastically different, as shows Fig. 5. The response at bias current 750 μA presented in Fig. 5(a) increases toward the boundaries of the array. At the right edge of the array the change of dissipation affects not only the velocity of the fluxons, but also the reflected radiation. The scan in Fig. 5(b) was measured at bias
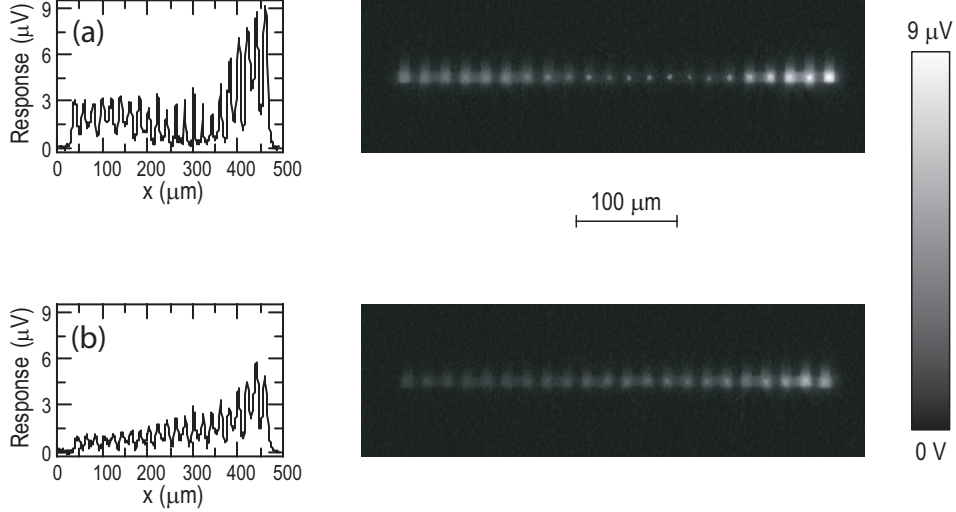

Figure 5: LTLSM voltage response of the SPA at the second resonance for bias current (a) 750 μA and (b) 800 μA

current 800 μA. At this point the response is smaller than that of at lower bias current, because the I-V curve here has a smaller differential resistance. Note that the maximum response regions for the first and second resonance branches are at the opposite ends of the array. At this point, we cannot exclude that this behavior is due to small deviations of the frustration from exactly one half.

At higher temperatures, 7.84 K, we have been mostly intersted in the bias current range for which we have detected large radiation power in our previous experiments [5, 7]. The scan in Fig. 6(a) corresponds to bias current of 600 μA and voltage 165 μV (open square in Fig. 2). This voltage is about the second resonance voltage at T=7.71 K. The scan is similar to the scan in Fig. 5(b). This result suggests that at 7.84 K the second resonance is not fully suppressed. The laser scanning at the high-voltage state ($I_{\mathrm{bias}} = 950\mu$A, open circle in Fig. 2) of the I-V curve shows a rather homogenous response (Fig. 6(b)). At this bias point the voltage of the array is already above the gap, where we would in fact expect to observe uniform signal.

In most of scans we see the pairs of the junctions. This occurs most probably due to the layout of our array. The paired junctions share the same top electrode. Neighboring not paired junctions share the same bottom electrode. We may expect that the top electrode is heated by the laser beam stronger than the bottom one. Because this heating is nonlocal, the heating of the top and bottom electrodes changes the parameters of neighboring junctions by different amount. On the other hand, our preliminary numerical simulation of the effect of low temperature scanning microscopy also show some pairing effect.
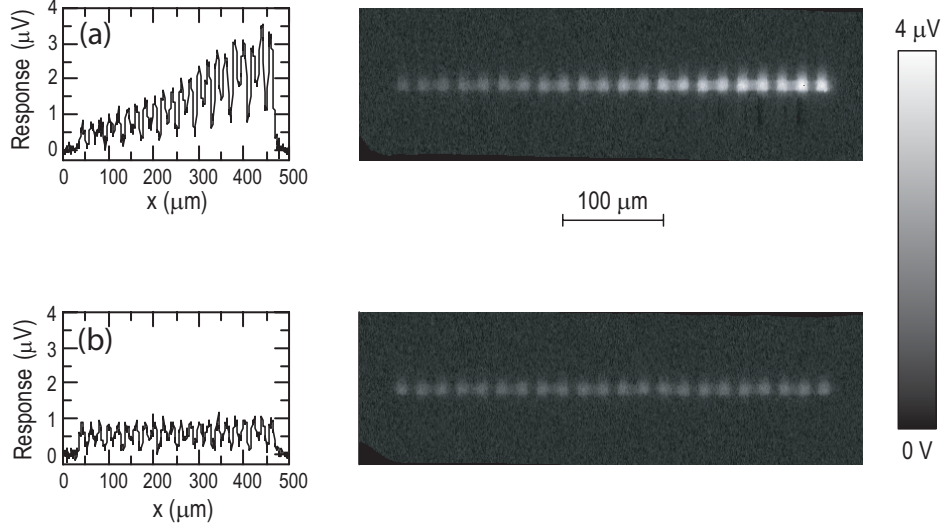
Figure 6: LTLSM voltage response of the SPA at the second resonance for bias current (a) 750 μA and (b) 800 μA at temperature 7.84 K

4   Conclusion

We reported here the LTLSM measurements of series-parallel Josephson junction arrays. For low damping case (low temperature) the array has two resonances. First, for bias points at first resonance the observed patterns show the largest response at the array boundary. These results show the array at the resonances operates in the similar manner as a long Josephson junction in the flux-flow regime. In the overdamped operation mode where the array shows the largest radiation power[5] the response is very uniform, as can be expected.

References

[1] D. Quenter, A.V. Ustinov, S.G. Lachenmann, T. Doderer, R.P. Huebener, F. Müller, J. Niemeyer, R. Pöpel and T. Weimann, Phys.Rev.B **51**, 6542 (1995)

[2] M.V. Fistul and A.V. Ustinov, Inst. Phys. Conf. Ser. No 167, p.177 (2000)

[3] A.K. Jain, K.K. Likharev, J.E. Lukens and J.E. Sauvageau Phys. Rep. **109**, 309 (1984)

[4] J. Bindslev Hansen and P.E. Lindelof, Rev. Mod. Phys. **56**, 431, (1984)

[5] A.A. Abdumalikov and A.V. Ustinov, Report No. 2 "Experiments on coupled Josephson junctions devices", contract F61775-01-W-E045 (2002)

[6] A.A. Abdumalikov, D. Abraimov and A.V. Ustinov, Report No. 2 "Testing of Josephson array antennas and trim current tuning", contract F61775-00-C0004 (2001)

[7] A.A. Abdumalikov and A.V. Ustinov, Report No. 3 "Experiments on coupled Josephson junctions devices", contract F61775-01-W-E045 (2002)

5   Final statement

(1) The Contractor, Prof. Dr. Alexey Ustinov, hereby declares that, to the best of its knowledge and belief, the technical data delivered herewith under Contract No. F61775-00-C0004 is complete, accurate, and complies with all requirements of the contract.

(2) I certify that there were no subject inventions to declare as defined in FAR 52.227-13, during the performance of this contract.

DATE: November 5, 2002

Name and Title of Authorized Official: Prof. Dr. Alexey Ustinov